Biochimica et Biophysica Acta 1849 (2015) 919–929

Contents lists available at ScienceDirect

Biochimica et Biophysica Acta

journal homepage: www.elsevier.com/locate/bbagrm

Epigenetic control of EMT/MET dynamics: HNF4α impacts DNMT3s through miRs-29☆,☆☆

Carla Cicchini [a,*,1], Valeria de Nonno [a,1], Cecilia Battistelli [a], Angela Maria Cozzolino [d], Marco De Santis Puzzonia [a], Silvia Anna Ciafrè [b], Chad Brocker [c], Frank J. Gonzalez [c], Laura Amicone [a], Marco Tripodi [a,d,**]

[a] Istituto Pasteur-Fondazione Cenci Bolognetti, Department of Cellular Biotechnologies and Hematology, Section of Molecular Genetics, Sapienza University of Rome, Rome, Italy
[b] Department of Biomedicine and Prevention, University of Rome Tor Vergata, Rome, Italy
[c] Laboratory of Metabolism, Center for Cancer Research, National Cancer Institute, National Institutes of Health, Bethesda, MD, USA
[d] National Institute for Infectious Diseases L. Spallanzani, IRCCS, Rome, Italy

ARTICLE INFO

Article history:
Received 17 November 2014
Received in revised form 17 April 2015
Accepted 13 May 2015
Available online 21 May 2015

Keywords:
De novo DNA methylation
Hepatocyte
Epithelial–mesenchymal transition
TGFβ
miR-29

ABSTRACT

Background and aims: Epithelial-to-mesenchymal transition (EMT) and the reverse mesenchymal-to-epithelial transition (MET) are manifestations of cellular plasticity that imply a dynamic and profound gene expression reprogramming. While a major epigenetic code controlling the coordinated regulation of a whole transcriptional profile is guaranteed by DNA methylation, DNA methyltransferase (DNMT) activities in EMT/MET dynamics are still largely unexplored.
Here, we investigated the molecular mechanisms directly linking HNF4α, the master effector of MET, to the regulation of both *de novo* of DNMT 3A and 3B.
Methods: Correlation among EMT/MET markers, microRNA29 and DNMT3s expression was evaluated by RT-qPCR, Western blotting and immunocytochemical analysis. Functional roles of microRNAs and DNMT3s were tested by anti-miRs, microRNA precursors and chemical inhibitors. ChIP was utilized for investigating HNF4α DNA binding activity.
Results: HNF4α silencing was sufficient to induce positive modulation of DNMT3B, in *in vitro* differentiated hepatocytes as well as *in vivo* hepatocyte-specific *Hnf4α* knockout mice, and DNMT3A, *in vitro*, but not DNMT1. In exploring the molecular mechanisms underlying these observations, evidence have been gathered for (i) the inverse correlation between DNMT3 levels and the expression of their regulators miR-29a and miR-29b and (ii) the role of HNF4α as a direct regulator of miR-29a-b transcription. Notably, during TGFβ-induced EMT, DNMT3s' pivotal function has been proved, thus suggesting the need for the repression of these DNMTs in the maintenance of a differentiated phenotype.
Conclusions: HNF4α maintains hepatocyte identity by regulating miR-29a and -29b expression, which in turn control epigenetic modifications by limiting DNMT3A and DNMT3B levels.

Abbreviations: ChIP, chromatin immunoprecipitation; DNMT, DNA methyltransferase; EMT, epithelial to mesenchymal transition; MET, mesenchymal to epithelial transition; TGFβ, transforming growth factor β; HNF4α, hepatocyte nuclear factor 4 alpha; qPCR, real-time polymerase chain reaction; RT–qPCR, reverse-transcription and real-time polymerase chain reaction

☆ Disclosures: All authors disclose any potential conflicts (financial, professional, or personal) that are relevant to the manuscript.

☆☆ Author contributions: C.C. designed the research plan, coordinated the experimental work, interpreted the results and wrote the manuscript; V.D.N. participated to the experimental design and the interpretation of results, and performed cell cultures and molecular analysis experiments; C.B. performed the ChIP experiments; A.M.C. performed molecular analysis experiments; M. D. S. P. performed immunofluorescence analysis; S.A.C. contributed to the critical revision; C. B. and F.J.G performed and coordinated the experimental work on mice; L.A. contributed to the critical revision; and M.T. designed the research plan, coordinated the experimental work, interpreted the results and wrote the manuscript.

* Correspondence to: C. Cicchini, Dipartimento di Biotecnologie Cellulari ed Ematologia, Sezione di Genetica Molecolare, *Sapienza* University of Rome, Viale Regina Elena 324, Rome 00161, Italy. Tel.: + 39 649918243; fax: + 39 64462891.

** Correspondence to: M. Tripodi, Dipartimento di Biotecnologie Cellulari ed Ematologia, Sezione di Genetica Molecolare, *Sapienza* University of Rome, Viale Regina Elena 324, Rome 00161, Italy. Tel.: +39 64461387; fax: +39 64462891.

E-mail addresses: cicchini@bce.uniroma1.it (C. Cicchini), tripodi@bce.uniroma1.it (M. Tripodi).

[1] These authors contributed equally to the work.

http://dx.doi.org/10.1016/j.bbagrm.2015.05.005

Table A.1
List and sequences of primers.

Target gene (*Mus musculus*)	Primer sequences (5′–3′)
Snail	*Fw* CCACTGCAACCGTGCTTTT
	Rev CACATCCGAGTGGGTTTGG
HNF4α	*Fw* TCTTCTTTGATCCAGATGCC
	Rev GGTCGTTGATGTAATCCTCC
DNMT3A	*Fw* CTGTCCCATCCAGGCAGT
	Rev CTTAGCGGTGTCTTGGAA
DNMT3B	*Fw* GCAAGACCTTCTCCAGCA
	Rev CTTGTTGGGTTTGAGGCCCT
DNMT1	*Fw* CCCAAAAGAAGGATCCTG
	Rev AGTTTGATGTCTGCCTCG
Occludin	*Fw* ACCTGATGAATTCAAACCCA
	Rev GTGAAGAATTTCATCTTCCGG
Mmp9	*Fw* CTTGAAGTCTCAGAAGGTGG
	Rev GGCTTTGTCTTGGTACTGG
E-cadherin	*Fw* CTACTGTTTCTACGGAGGAG
	Rev CTCAAATCAAAGTCCTGGTC
Vimentin	*Fw AGCAGTATGAAAGCGTGGCT*
	Rev CTCCAGGGACTCGTTAGTGC
β-actin	*Fw* ACCACACCTTCTACAATGAG
	Rev AGGTCTCAAACATGATCTGG
U6	*Fw* GCTTCGGCAGCACATATACT
	Rev GAATTTGCGTGTCATCCTTG
mmu-miR-29a	*Fw* T*GC*C*ATCTGAAAT (*LNA)
	Rev AACTGCGGATTATCGAACTAT
mmu-miR-29b	*Fw* T*AG*CA*CCATTTGAAA (*LNA)
	Rev TTTGAACATAGATTGGGCTC
18S	*Fw* ACGACCCATTCGAACGTCTG
	Rev GCACGGCGACTACCATCG
L34	*Fw* GGAGCCCCATCCAGACTC
	Rev CGCTGGATATGGCTTTCCTA
Snord66	*Fw* G*C*GTGCCACGTGT (*LNA)
	Rev CCACAGCCATAGTCAGTACAAGGTCCTC

1. Introduction

The execution of epithelial cells' specific functions, guaranteed by differentiated phenotypes, includes the capacity to respond to environmental cues that trigger mesenchymal transdifferentiation. This pleiotropic process known as epithelial-to-mesenchymal transition (EMT), manifestation of plasticity by a deep and dynamic gene expression reprogramming, is often followed by the reverse mesenchymal-to-epithelial transition (MET), occurring in a secondary site and in a different cellular environment. EMT/MET dynamics occur in both physiological phenomena, such as organogenesis, development, wound healing and regeneration, and pathological conditions. The aberrant acquisition of mesenchymal characteristics by epithelial cells, with the loss of apical-basal polarity and the enhanced migratory capacity, characterizes fibrosis, tumor progression and metastasis [1].

Epigenetic mechanisms are conceivably mandatory in allowing the execution of such a deep and dynamic cellular reprogramming that involves the coordinated regulation of a whole transcriptional profile.

A major epigenetic code controlling gene expression is guaranteed by DNA methylation orchestrated by DNA methyltransferases 1 (DNMT1) and 3 (DNMT3A and DNMT3B) [2]. Current knowledge indicates that while DNMT1 is primarily involved in the maintenance of an established DNA methylation pattern [3], the DNMT3s possess an efficient *de novo* methylation activity necessary to determine new methylation patterns required during development [4]. The aberrant modification of epigenetic marks also characterizes various malignancies and, in particular, the levels of DNMTs are elevated in several cancers including hepatocarcinoma (HCC) [5,6]. Specifically in HCC, changes in cytosine methylation were suggested as possible molecular markers for tumor progression while treating HCC cells with the DNMT inhibitor decitabine reduced invasiveness [7,8].

DNA methylation in EMT/MET dynamics is still largely unexplored and evidence are mainly limited to the inverse correlation found between DNA methylation and transcription levels of EMT/MET key markers [9–11] and to the whole genome EMT-associated DNA methylation changes [12]. Moreover, the molecular mechanisms directly linking master effectors of EMT/MET to DNA methylation by DNMTs are still not unveiled.

Wide evidence demonstrated that the orphan nuclear receptor hepatocyte nuclear factor 4-α (HNF4α), master regulator of hepatocyte differentiation and hepatic epithelium formation [13,14], also acts as a master regulator of MET (for review [15]). Notably, a role for HNF4α as a direct repressor of master EMT regulators and mesenchymal genes was recently unveiled, thus providing evidence for its pivotal function for both the regulation of the dynamic process of MET and the maintenance of a stable epithelial phenotype [16].

Here, the HNF4α role in the maintenance of hepatocyte epithelial identity is linked to the epigenetic modifications featured by *de novo* DNMT3A and DNMT3B. HNF4α silencing in differentiated hepatocytes was, in fact, found sufficient to induce both DNMT3A and DNMT3B positive modulation *in vitro* and DNMT3B *in vivo*, while DNMT1 levels were unchanged. Exploring the molecular mechanisms underlying these observations, evidence for (i) the inverse correlation among the levels of DNMT3A and DNMT3B and the expression of miR-29a and miR-29b, targeting their transcripts [17] and (ii) the role for HNF4α as direct regulator of these microRNA transcription have been gathered. Notably, during the transforming growth factor β (TGFβ)-induced EMT of differentiated hepatocytes, DNMT3 up-regulation was found to occur and its function in this process suggested.

2. Materials and methods

2.1. Cell culture conditions

Untransformed differentiated hepatocytes [18] were grown in RPMI 1640 with 10% FBS (GIBCO® Life Technology, Monza, Italy), 50 ng/ml EGF, 30 ng/ml IGF II (PeproTech Inc., Rocky Hill, NJ, USA), 10 μg/ml insulin (Roche, Mannheim, Germany) and antibiotics, on collagen I (GIBCO® Life Technology, Monza, Italy) coated dishes. When indicated, cells were treated with 5 μM TGFβ1 for 24 h (PeproTech Inc., Rocky Hill, NJ, USA), according to [19], and/or with 4 μM DNA-methyltransferases inhibitor 5-Azacytidine (5-Aza; Sigma-aldrich, Sant Louis, MO, USA).

2.2. Animal model and treatment

Conditional temporal $Hnf4a^{F/F;AlbERT2cre}$ mice used in this study were previously described (PMID: 22241473). In brief, $Hnf4a^{F/F}$ mice were crossed with $SA^{+/Cre\text{-}ERT2}$ mice expressing a tamoxifen-inducible, hepatocyte-specific Cre recombinase (PMID: 15282742 & 21725089). Cre recombinase expression and subsequent gene knockout were induced by feeding a diet containing tamoxifen (1 g/kg diet) for 4 days. Mice were returned to regular chow for an additional 4 days then euthanized and livers were excised for subsequent studies. The mice were on a mixed SvJ129/FVB background and used at 8–10 weeks of age. All mice were given food and water *ad libitum* and housed in a light- and temperature-controlled facility. All animal studies were performed in accordance with the guidelines and approval of the National Cancer Institute, National Institutes of Health, Animal Care and Use Committee.

2.3. siRNA interference

Cells were transfected with equal amounts of small interfering RNA (siRNA) oligonucleotides against GFP (5′-GGC UAC GUC CAG GAG CGC ACC-3′), as control, or against HNF4α (ON-TARGET plus SMART pool siRNAs J-065463-05/06/07/08, Dharmacon, Lafayette, CO) or against DNMT3A (ON-TARGET plus SMART pool siRNAs J-065433-09/10/11/12, Dharmacon, Lafayette, CO) and DNMT3B (ON-TARGET plus SMART

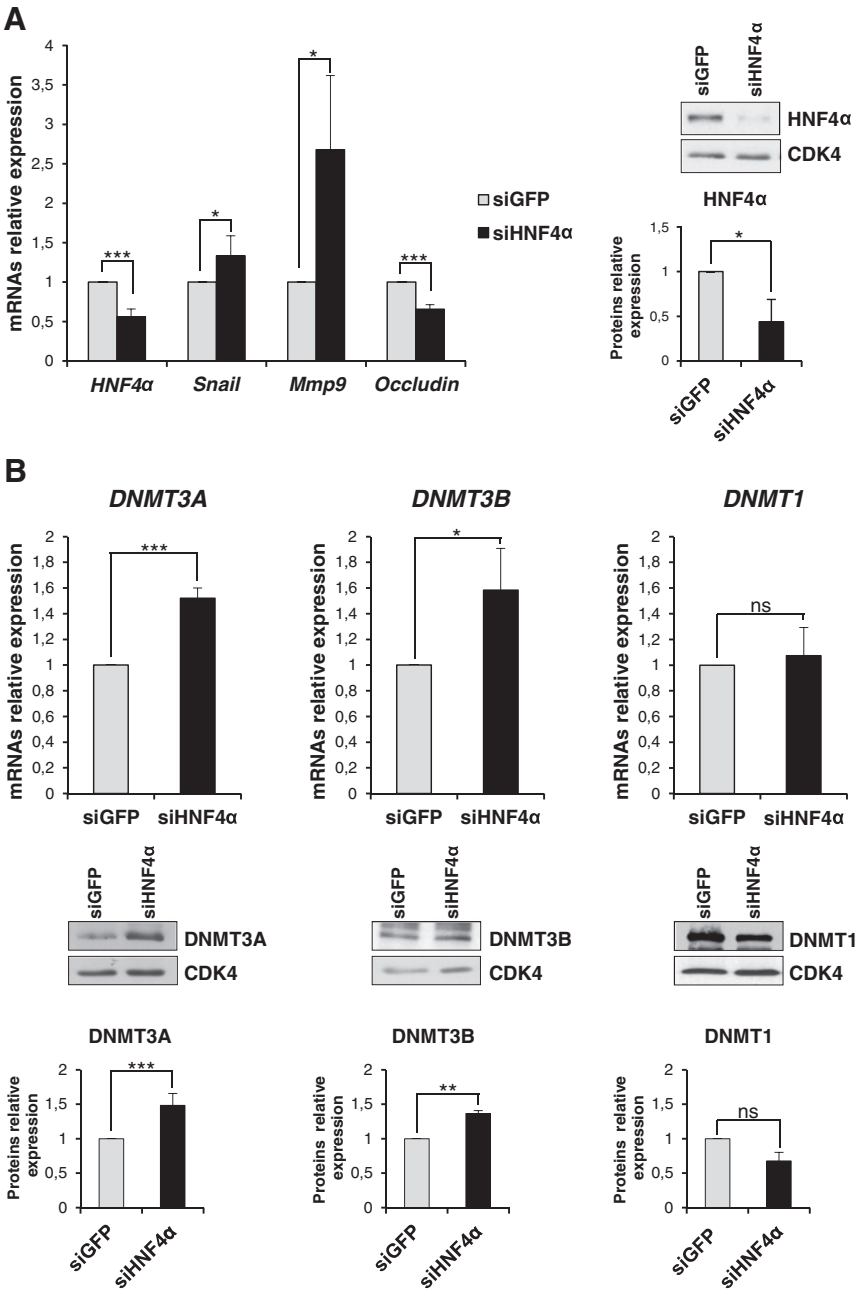

Fig. 1. HNF4α silencing induces DNMT3A and DNMT3B in hepatocytes. (A) Left panel: RT-qPCR analysis for the indicated genes in HNF4α silenced (for 48 h) (siHNF4α), compared to control siGFP cells. The values are calculated by ΔΔCt method and expressed as relative versus the control (arbitrary value = 1). Right panel: Western blot and densitometric analysis on total protein extracts from siHNF4α and siGFP cells. WB figures represent one indicative experiment of three independent ones. Densitrometic values of protein amounts normalized by immunoblotting for CDK4 are expressed as fold of expression vs the control (siGFP). Statistically significant differences are reported (*$p < 0.05$, ***$p < 0.001$) for three independent experiments. RT-qPCR (upper panels) and Western blot (middle panels) analysis for the indicated markers in siHNF4α and siGFP cells. Densitometric analysis (lower panels) and statistically significant differences (*$p < 0.05$, **$p < 0.01$, ***$p < 0.001$; n.s. no significance) for three independent experiments are reported. Protein amount was normalized by immunoblotting for CDK4 and WB figures represent one indicative experiment of three independent ones. (B) Western blot analysis for the indicated markers on protein extracts from 6 hepatocyte-specific *Hnf4α* knockout (KO) mice (*Hnf4α*$^{F/F;AlbERT2cre}$; PMID: 22241473) and 6 matched Cre negative littermates (*Hnf4α*$^{+/+}$). Protein amount was normalized by immunoblotting for α-β actin, as indicated. Densitometric analysis and statistically significant differences (**$p < 0.01$; ***$p < 0.001$; n.s. no significance) are reported.

pool siRNAs J-044164-05/06/07/08, Dharmacon, Lafayette, CO) by Lipofectamine 2000 (Invitrogen, San Diego, CA, USA) according to commercial protocol. Samples have been collected 48 h after transfection and analyzed for transcripts and/or proteins levels.

2.4. Transfection of miR precursors and inhibitor treatment

miRs-29a and 29b knock down and miR-29b overexpression were obtained respectively by the use of specific commercial anti-miR inhibitors and a pre-miR precursor oligonucleotide, or the corresponding amount of negative controls, purchased by Ambion® (AM17110, AM17010, AM12499, AM10103 and PM10103, Life Technology, Monza, Italy). Transfections were performed by Lipofectamine 2000 (Invitrogen, San Diego, CA) according to commercial protocol and analysis performed after 48 h. Cells were transfected with a pool of anti-miR-29a and anti-miR-29b, or the corresponding negative control, and interfered after 24 h by control siRNAs (siGFP) or siRNAs specific for DNMT3A and DNMT3B (siDNMT3s). Samples were collected and molecular analysis performed after the successive 48 h.

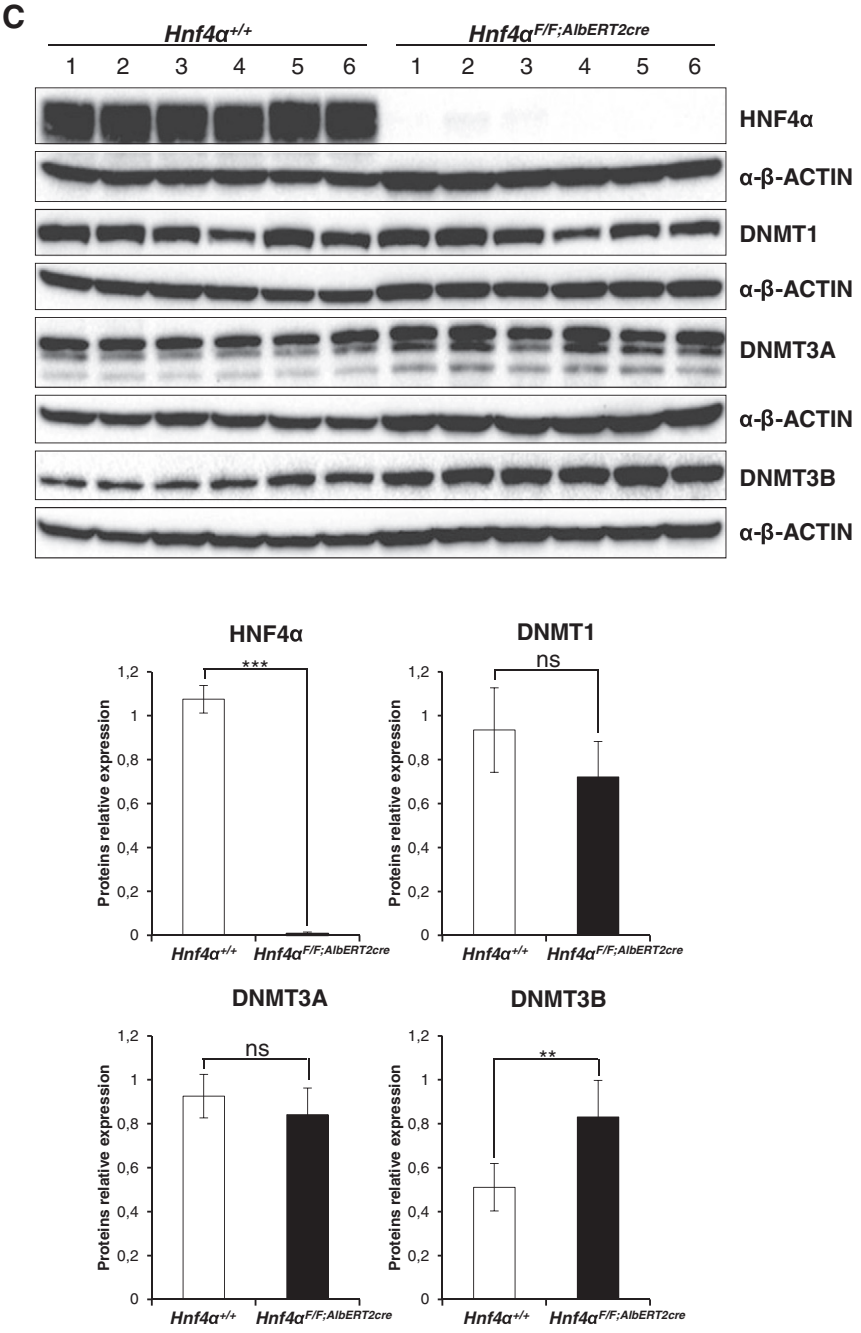

Fig. 1 (*continued*).

2.5. RNA extraction, reverse transcription (RT), reverse-transcription and real-time polymerase chain reaction (RT–qPCR)

Total RNA was extracted by cell cultures and liver samples by TRIzol (Invitrogen, Carlsbad, CA) or miRNeasy Mini Kit (QIAGEN GmbH, Hilden, Germany) and reverse transcribed by iScript™ c-DNA Synthesis Kit (Bio-Rad Laboratories, Inc., Hercules, CA, USA). For miRs retrotranscription, the cDNA was obtained by reverse transcription of total RNA (200 ng), using Superscript III reaction kit (Invitrogen, Carlsbad, CA, USA), and amplified by qPCR reaction using GoTaq® qPCR Master Mix (Promega, Madison, WI, USA). Relative amounts were obtained with $2^{-\Delta\Delta Ct}$ method and normalized to β-actin, L34 or 18S (microRNA normalized for U6 or Snord66). Specific primers are listed in Table A.1.

2.6. Western blot

Cells were lysed in RIPA buffer (50 mM Tris–HCl pH 8.0, 150 mM NaCl, 1 mM EDTA, 100 mM NaF, 3 mM Na orthovanadate, 10% glycerol, 1% NP-40), supplemented with protease inhibitors (complete EDTA-free, Roche Applied Science, Mannheim Germany), and proteins quantified by Bradford protein assay reagent (Bio-Rad Laboratories, Hercules, CA, USA). Equal amounts of proteins were separated by SDS-PAGE and transferred onto nitrocellulose membrane (HybondTM ECLTM; GE Healthcare, Freiburg Germany). Blots were blocked in 5% non-fat milk prepared in TBST and incubated overnight at 4 °C with the primary antibodies (antibodies α-HNF4α (C-19, sc-6556 1:500), α-CDK4 (C-22, sc-260 1:1000), α-TUBULIN (TU-02, sc-8035 1:1000), α-DNMT3A

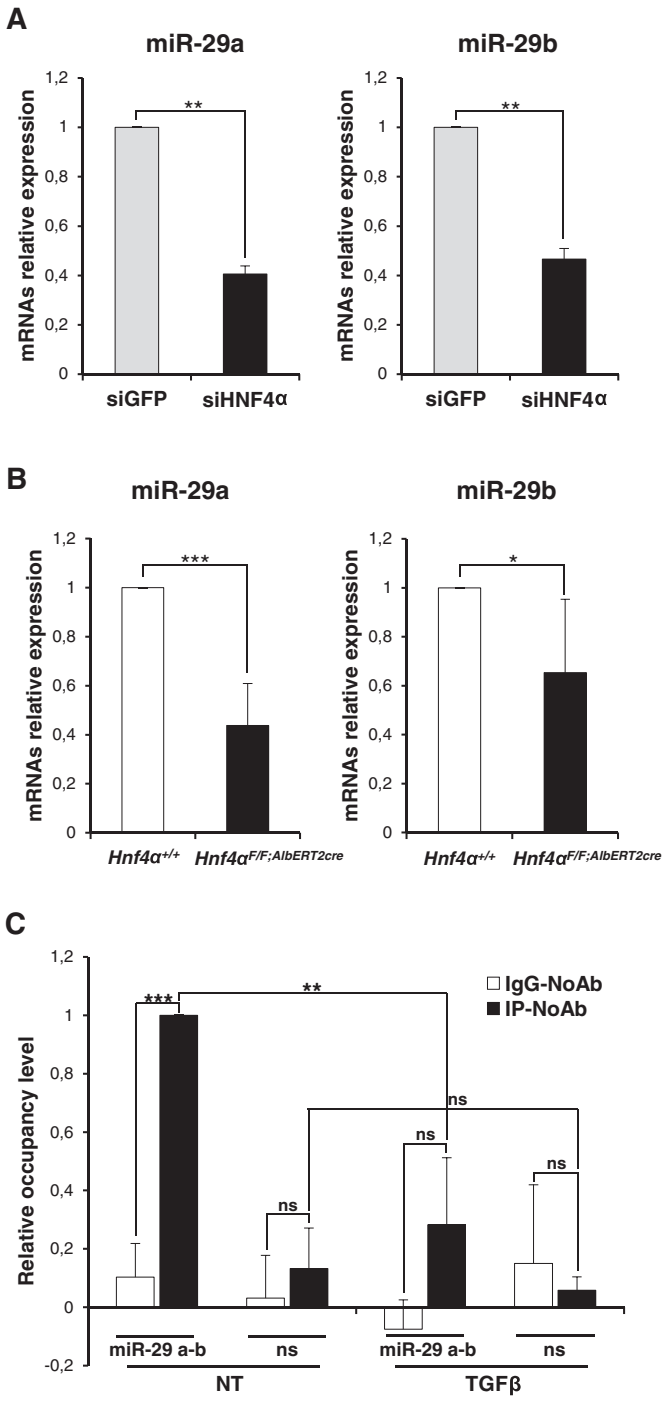

Fig. 2. HNF4α controls the expression of miR-29a and miR-29b. (A) RT-qPCR analysis for the indicated murine microRNAs on siHNF4α and siGFP cells as in Fig. 1. The values are calculated by ΔΔCt method and expressed as relative versus the control (arbitrary value = 1). Statistically significant differences are reported (**$p < 0.01$) for three independent experiments. (B) RT-qPCR analysis for the indicated miRs on liver samples from 5 hepatocyte specific HNF4α KO mice (*Hnf4α* $^{F/F;AlbERT2cre}$; PMID: 22241473) and 5 matched Cre negative littermates (*Hnf4α*$^{+/+}$). Values are calculated by ΔΔCt method and statistically significant differences are reported (*$p < 0.05$, ***$p < 0.001$). (C) qPCR analysis of ChIP assays with an anti-HNF4α antibody, or normal rabbit IgG as negative control, on chromatin from cells treated (TGFβ) or not (NT) with TGFβ for 24 h, showing the direct recruitment of endogenous HNF4α on the miR-29a-b promoter. ChIP on specific HNF4α consensus (miR-29 a–b) compared with non-specific genomic region (ns) are both normalized to total chromatin input and expressed as (IP-NoAb), shown in dark bars, and (IgG-NoAb), shown in white bars. Statistically significant differences are reported (**$p < 0.01$; ***$p < 0.001$; n.s. no significance) for three independent experiments.

(H-295, sc-20703 1:1000) and α-DNMT3B (H-230, sc-20704 1:1000) were purchased from Santa Cruz Biotechnology (Santa Cruz Biotechnology, CA, USA); α-Snail antibody (L70G2, 1:1000) from Cell Signaling Technology® (Danvers, MA, USA)) and α-DNMT1 antibody (60B1220.1, 1:1000) from Novus Biologicals (Littleton, CO, USA). Blots were incubated with HRP-conjugated anti-Mouse and Rabbit secondary antibodies (170-6516 and 172-1019, Bio-Rad Laboratories, Inc., Hercules, CA, USA) or with HRP-conjugated anti-Goat IgG (705-036-147 1:5000, Jackson Immuno Research Laboratories, Inc., West Grove, PA, USA) followed by enhanced chemiluminescence reaction (WESTAR NOVA 2011 or ηC, Cyanagen, Bologna, Italy).

The impressed X-ray films were submitted to densitometric analysis by using ImageJ open source software (release 1.44p, http://imagej.nih.gov/ij). Values were expressed as specific protein signal/loading control signals (TUBULIN or CDK4, as indicated) and reported as fold of expression.

For liver samples, tissues were lysed in RIPA buffer containing protease inhibitors using a Precellys 24 homogenizer. Lysates were cleared by centrifugation and protein concentrations quantified using Pierce BCA Assay Kit (Thermo Scientific, Waltham, MA USA). Samples were ran on pre-cast Criterion TGX gels and transferred to PVDF using TransBlot Turbo transfer system (BioRad, Hercules, California, USA). Following transfer, blots were processed as described above using primary antibodies (α-HNF4α (H1415, PP-H1415-00 1:10K) from R&D Systems (Minneapolis, MN, USA); α-DNMT3A (H-295, sc-20703 1:1000) and α-DNMT3B (H-230, sc-20704 1:1000) from Santa Cruz Biotechnology; α-DNMT1 antibody (60B1220.1, 1:1000) from Novus Biologicals (Littleton, CO, USA) and α-β-actin (Ab8227 1:10K) from Abcam (Cambridge, MA, USA)). Blots were incubated with HRP-conjugated anti-Mouse (#7076, 1:5K) or anti-Rabbit (SC-7054) secondary antibodies from Cell Signaling Technology and Santa Cruz Biotechnology, respectively. Chemiluminescence detection was carried out using Clarity Western ECL Substrate (BioRad) and a ChemDoc MP system (BioRad).

2.7. Immunofluorescence analysis

For indirect immunofluorescence analysis, cells were fixed in 4% paraformaldehyde and permeabilized with Triton-X100. The following primary antibodies were used: anti-Snail rabbit polyclonal (ab180714 Abcam Cambridge UK) 1/50, anti-MMP9 rabbit monoclonal (ab1378867, Abcam Cambridge UK) 1/50, anti-Vimentin rabbit monoclonal (ab92547, Abcam Cambridge UK) 1/400, and anti-E-cadherin mouse monoclonal (BD 610182 BD Biosciences Pharmingen, Palo Alto, CA, USA) 1/50. Secondary antibodies (anti-mouse Alexa-Fluor 594, anti-rabbit Alexa-Fluor 488; 1/400) were from Molecular Probes (Eugene, OR, USA). DNA has been stained by DAPI (Santa Cruz Biotechnology, Inc., CA, USA). Preparations were examined under Nikon Eclipse fluorescent microscope equipped with a 20× (0.9 NA) and a CCD camera (Nikon Inc.). Digital images were processed with Adobe Photoshop 7 software (Adobe Systems, Mountain View, CA). The same enhanced color levels were applied for the green channel.

2.8. Chromatin immunoprecipitation (ChIP) analysis

ChIP analysis was performed as previously reported [19] by using 5 μg rabbit anti-HNF4α (H-171, sc-8987; Santa Cruz Biotechnology, Inc., CA, USA) or the negative control normal rabbit IgG (SC-2027; Santa Cruz Biotechnology, Inc., CA, USA). 5 ng of immunoprecipitated DNA and the relative controls were used as templates for real time qPCR analysis, performed in triplicate. Primers are reported: *HNF4α consensus on miR-29a-b promoter* forward 5′-TTGTCGACTCTAACAGATCG-3′ and reverse 5′-GAGCACGAGGCTTACACATT-3′. *Non-specific genomic control region* (TIMM17) forward 5′-ACGGATGTGGCCCTTCTGGCT-3′ and reverse 5′-CCGCTCCGAAACGCCCACAA-3′. ChIP analyses (by

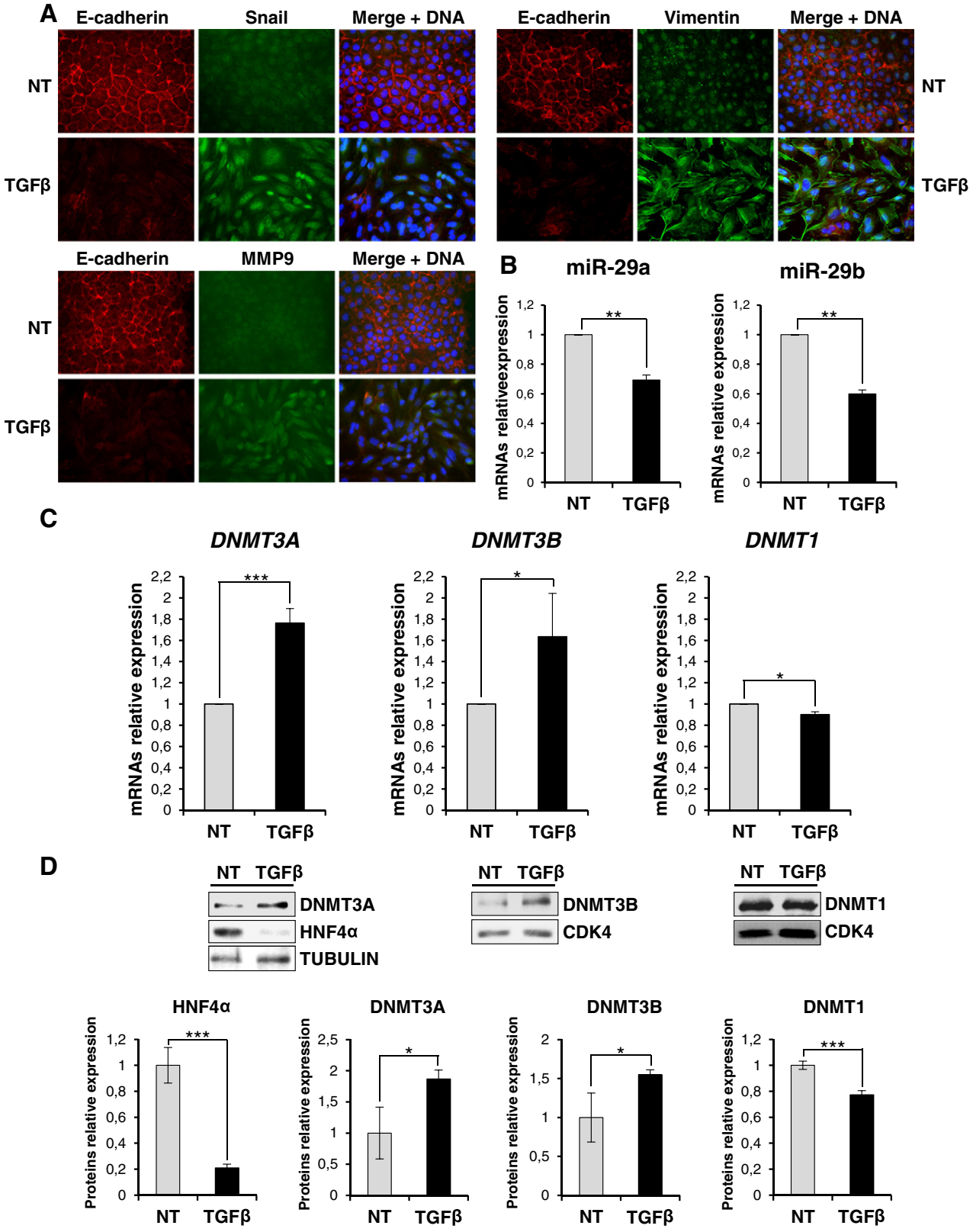

Fig. 3. TGFβ treatment induces DNMT3A and DNMT3B in hepatocytes. (A) Immunofluorescence analysis for the indicated epithelial (E-cadherin) and mesenchymal (Snail, Vimentin, MMP9) markers for cells treated (TGFβ) or not (NT) with TGFβ for 24 h (magnification ×20). Blue DAPI staining shows nuclei (DNA). (B) RT-qPCR analysis for the indicated miRs in cells treated as in (A). The values are calculated by the ΔΔCt method and expressed as relative versus the controls (arbitrary value = 1). Statistically significant differences are reported (**$p < 0.01$) for three independent experiments. (C) RT-qPCR analysis for the indicated markers on total RNA for cells as in (A). Statistically significant differences are reported (*$p < 0.05$, ***$p < 0.001$) for three independent experiments. (D) Western blot analysis for the indicated markers on protein extracts for cells as in (A). Protein amount was normalized by immunoblotting for CDK4 or tubulin, as indicated. Figures represent one indicative experiment of three independent ones. Densitometric analysis and statistically significant differences (*$p < 0.05$, ***$p < 0.001$) for three independent experiments are reported.

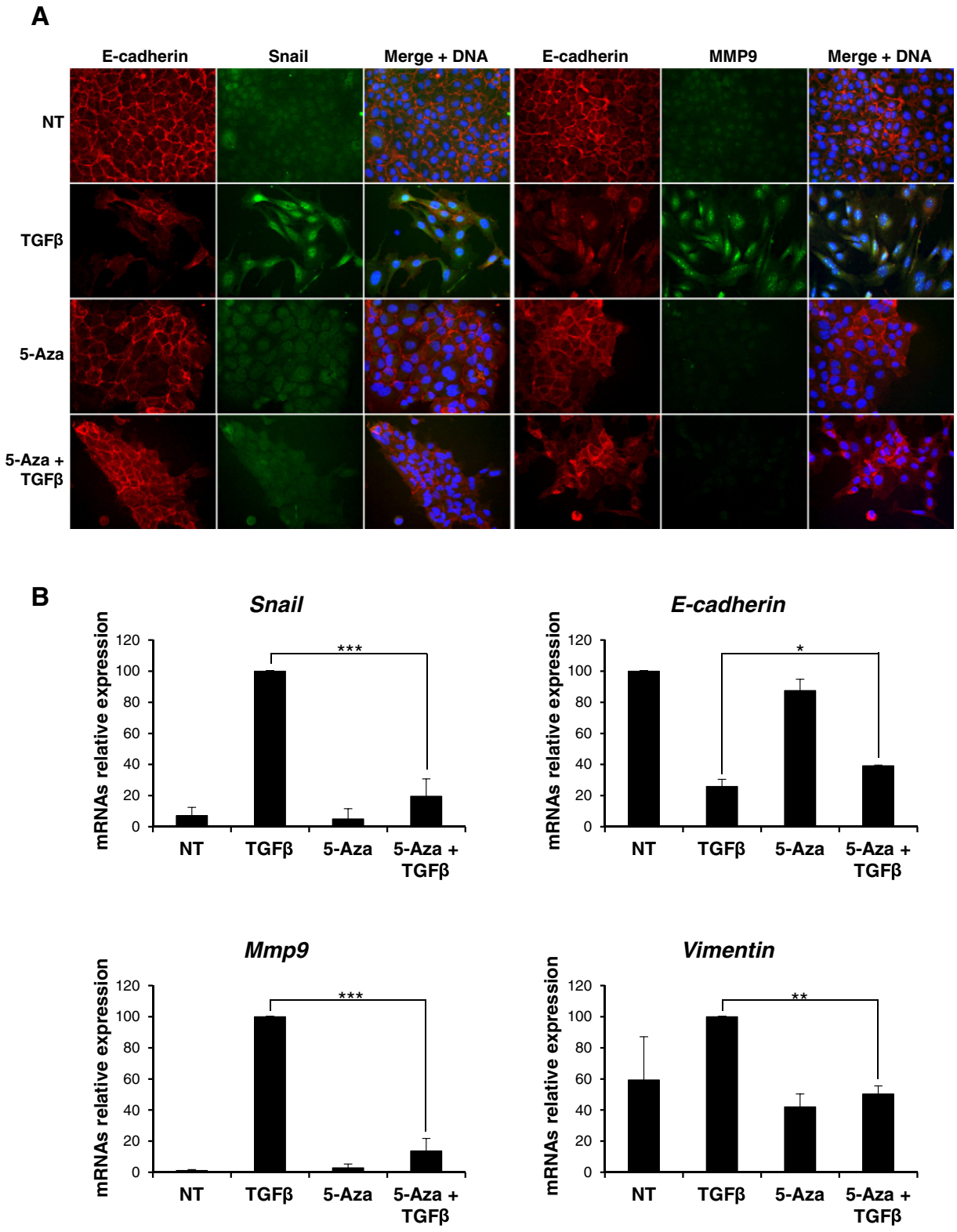

Fig. 4. DNMTs are required in TGFβ-mediated EMT induction. (A) Immunofluorescence analysis for the indicated epithelial (E-cadherin) and mesenchymal (Snail, MMP9) markers for cells treated or not (NT) for 72 h with 5-Azacytidine (5-Aza), 24 h with TGFβ (TGFβ) or both (5-Aza + TGFβ)(magnification ×20). Blue DAPI staining shows nuclei (DNA). (B) RT-qPCR analysis for *Snail*, *E-cadherin*, *Mmp9* and *Vimentin* expressions on cells grown as in (A). The values are calculated by ΔΔCt method and expressed as relative versus the controls (arbitrary value = 1) Statistically significant differences are reported (*$p < 0.05$, **$p < 0.01$, ***$p < 0.001$) for three independent experiments.

HNF4α antibody (IP) or IgG (IgG)) on specific HNF4α consensus, compared with non-specific genomic regions (ns), were both normalized to total chromatin input and expressed as (IgG-NoAb) and (IP-NoAb).

2.9. Statistical analysis

Student's t test was used for statistical analyses. All the tests were two-sided and a p-value < 0.05 was considered statistically significant

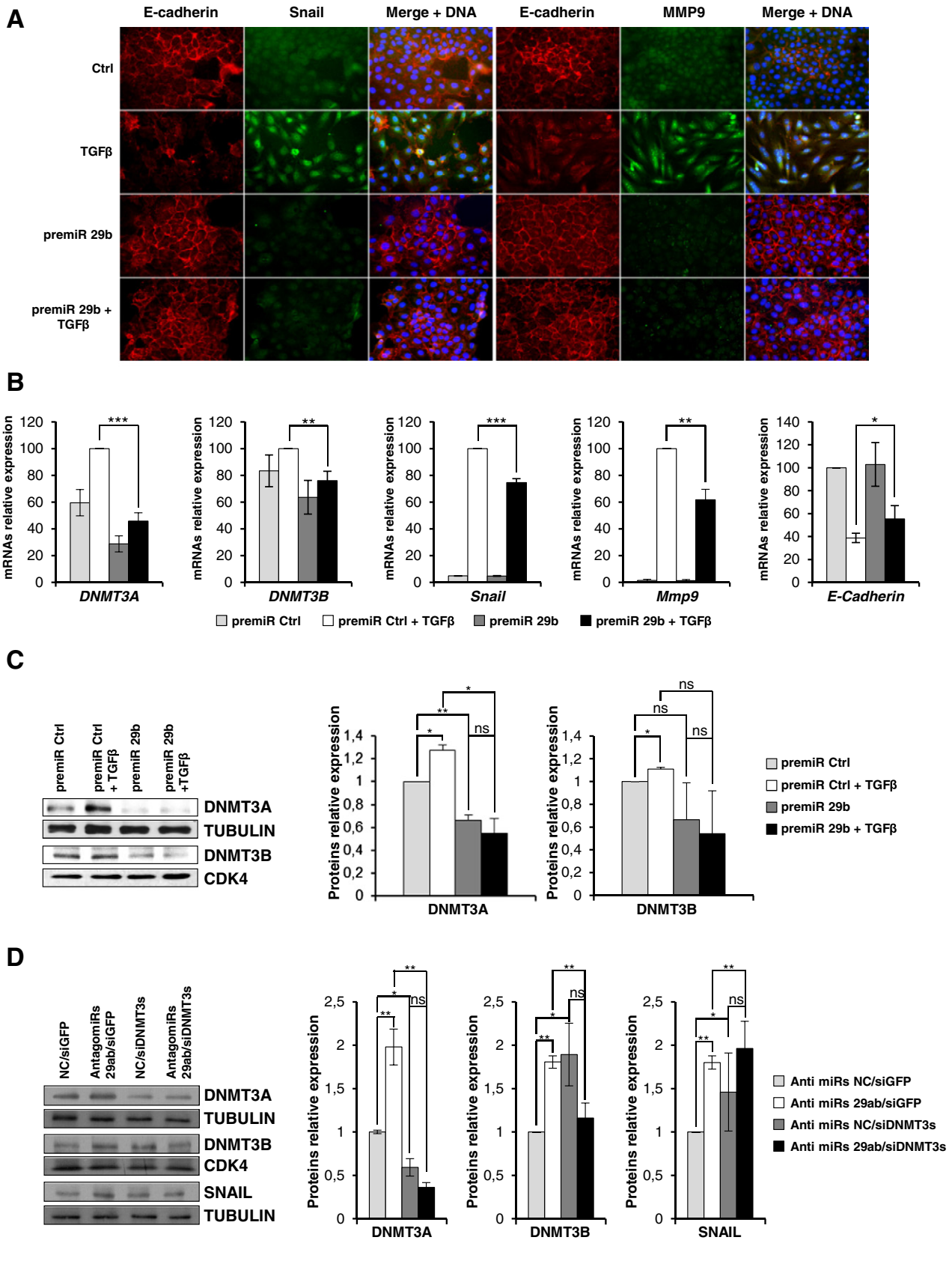
A
E-cadherin
Snail
Merge + DNA
E-cadherin
MMP9
Merge + DNA
Ctrl
TGFβ
premiR 29b
premiR 29b + TGFβ
B
mRNAs relative expression
DNMT3A
DNMT3B
Snail
Mmp9
E-Cadherin
premiR Ctrl
premiR Ctrl + TGFβ
premiR 29b
premiR 29b + TGFβ
C
premiR Ctrl
premiR Ctrl + TGFβ
premiR 29b
premiR 29b +TGFβ
DNMT3A
TUBULIN
DNMT3B
CDK4
Proteins relative expression
DNMT3A
DNMT3B
ns
D
NC/siGFP
AntagomiRs 29ab/siGFP
NC/siDNMT3s
AntagomiRs 29ab/siDNMT3s
DNMT3A
TUBULIN
DNMT3B
CDK4
SNAIL
TUBULIN
Proteins relative expression
DNMT3A
DNMT3B
SNAIL
Anti miRs NC/siGFP
Anti miRs 29ab/siGFP
Anti miRs NC/siDNMT3s
Anti miRs 29ab/siDNMT3s

(pairs of samples marked with * symbol). Where the statistical significance was higher additional marks were added (p-value < 0.01 = **, p-value < 0.001 = ***).

2.10. Bioinformatic analysis

Regulatory sequence (up to 1 kb upstream of transcription start site) of murine microRNA-29a-b was obtained from ENSEMBL (http://www.ensembl.org) and submitted to MatInspector Professional (release 8.0, Genomatix, Munchen, Germany), using the vertebrate matrix library and optimized thresholds, to identify putative HNF4α binding sites.

3. Results

3.1. HNF4α impairment induces DNMT3A and DNMT3B expression

In order to identify a conceivable link between the master regulator of MET, HNF4α, and epigenetic modifications, we first focused on the DNA methylation machinery and analyzed DNMT1, DNMT3A and DNMT3B expression in differentiated hepatocytes in which HNF4α has been knocked-down. In these cells, the HNF4α interference by siRNAs (Fig. 1A) was previously found sufficient to determine the loss of the hepatocyte differentiated phenotype and the expression of several mesenchymal genes under the control of this transcriptional regulator. In particular, HNF4α has been proven to act as a pivotal element in maintaining a differentiated epithelial state by acting as a direct repressor of Snail, Slug and HMG1, the main inducers of EMT [16].

Here, once monitored that HNF4α silencing induced both the master regulator *Snail* and the mesenchymal marker metalloprotease-9 (*Mmp9*) and caused the repression of the epithelial marker Occludin (Fig. 1A; as expected according to [16]), we investigated on DNMTs: as shown in Fig. 1B, in HNF4α interfered cells DNMT3A and DNMT3B, but not DNMT1, were found up regulated at their transcript and protein levels.

In extending our observations to an *in vivo* model, hepatocyte-specific *Hnf4α* knockout (KO) mice (*Hnf4a*$^{F/F;AlbERT2cre}$; PMID: 22241473) and matched Cre negative littermates (*Hnf4a*$^{F/F)}$ were analyzed for DNMT expression. DNMT3B was significantly up regulated in all KO mice with respect to littermates, while levels of DNMT1 and DNMT3A were variable within each group (Fig. 1C). DNMT3A up regulation was observed in half of the animals examined, however, densitometry analysis did not indicate statistical significance (Fig. 1C).

In particular, it is here worth recalling that hepatocytes from HNF4α KO mice were also previously shown to exhibit a marked induction of Snail and of the mesenchymal proteins desmin, vimentin, and a-smooth muscle actin, highlighting the requirement of HNF4α in maintaining the hepatocyte epithelial identity [16].

Overall, these data provide evidence that the HNF4α impairment in hepatocytes, previously reported to cause the acquisition by the hepatocyte of mesenchymal traits [16], is sufficient to induce *de novo* DNA methyltransferases DNMT3B (both in the cell culture and in the animal models) and DNMT3A (only in the in vitro model) up-regulation.

3.2. MicroRNA-29a and 29b, targeting DNMT3A and DNMT3B, are regulated by HNF4α

Previous studies demonstrated that miR-29 family members efficiently target DNMT3A and DNMT3B transcripts in different cell systems [17]. Another study revealed that miR-29a-mediated regulation of DNMT is involved in TGFβ-induced EMT of transformed cells [20]. In order to gain insight into a possible mechanism of DNMT3 isoform modulation by HNF4α, we investigated microRNA-29a and microRNA-29b expression in HNF4α-interfered hepatocytes. As shown in Fig. 2A and B, miR-29a and miR-29b were both found expressed in differentiated hepatocytes and, notably, highly correlating to HNF4α expression; HNF4α silencing in cells, in fact, caused a strong decrease of their levels, while in *in vivo* knockout a marked decrease was observed for miR-29b only. Finally, since our bioinformatic analysis *via* MatInspector revealed putative HNF4α binding sites on the miR-29a and miR-29b shared promoter, we investigated the possible direct control of miR-29s expression by this master regulator. Chromatin immunoprecipitation (ChIP) analysis (Fig. 2C) showed the direct recruitment of endogenous HNF4α on the miR-29a-b promoter in hepatocytes, in which miRs-29 are expressed, and its displacement during EMT, when its activity is impaired by TGFβ and miRs-29 are repressed [21,16]. Overall, our results suggest that HNF4α is directly involved in the induction of miR-29a and -29b expression, thus impairing *de novo* DNA methylation in differentiated hepatocytes.

3.3. DNMT3A and DNMT3B are required in TGFβ-induced EMT

Data so far illustrated and obtained in differentiated hepatocytes may be interpreted as a mechanism that antagonizes epigenetic modifications and stabilizes the hepatocyte epithelial phenotype. In order to investigate the functional requirement for a *de novo* DNA methylation in the dynamic of hepatocyte EMT, we analyzed DNMT3 expression during the transition.

As shown in Fig. 3 (and in line with a previous report [19]), tgfβ treatment induced an EMT, as judged by immunofluorescence analysis of mesenchymal (i.e. Snail, MMP9, Vimentin) and epithelial (E-cadherin) markers (Fig. 3A); notably, in these conditions an inverse correlation between mir-29a and mir-29b expression and DNMT3A and DNMT3B (but not DNMT1), at both transcriptional and protein levels, was observed (Fig. 3B–C–D). In order to evaluate whether the *de novo* DNA methyltransferase modulation in tgfβ-induced EMT was only correlative or rather causal to the transition, we analyzed the effects of its inhibition. To this aim, cells were treated with the inhibitor 5-Azacytidine (5-Aza), a nucleotide analog that is incorporated into DNA, where it produces an irreversible inactivation of DNA methyltransferases [22]. As shown in Fig. 4A, immunofluorescence analysis in control tgfβ-treated hepatocytes highlighted i) acquisition of a fibroblastic phenotype with MMP9 induction, ii) Snail nuclear staining and iii) E-cadherin delocalization and down regulation. Conversely, cells co-treated with tgfβ and 5-Aza still retained an epithelial morphology with membrane staining of E-cadherin. Coherently, quantitative qrt-PCR analysis showed that tgfβ treatment of 5-Aza-treated cells did not cause a significant *Snail* induction and, consequently, did not cause

Fig. 5. miR-29b overexpression interferes with TGFβ-mediated EMT. (A) Immunofluorescence analysis for the indicated epithelial (E-cadherin) and mesenchymal (Snail, MMP9) markers for cells overexpressing a negative control microRNA precursor (Ctrl) or the same amount of a pre-miR-29b and either treated or not with TGFβ for 24 h (magnification ×20). Blue DAPI staining shows nuclei (DNA). (B) RT-qPCR analysis for the indicated genes on cells in the same conditions as above. The values are calculated by ΔΔCt method and expressed as above. Data are expressed as mean ± SD of triplicate samples. Statistically significant differences are reported (*p < 0.05, **p < 0.01, ***p < 0.001) for three independent experiments. (C) Western blot analysis for the indicated markers of total protein extracts from cells in the same conditions as above. Protein amount was normalized by immunoblotting for CDK4 or tubulin, as indicated. Figures represent one indicative experiment of three independent ones. Densitometric analysis and statistically significant differences (*p < 0.05, **p < 0.01, n.s. no significance) for three independent experiments are reported. (D) Western blot analysis and densitometric analysis for the indicated markers on cells transiently transfected with the negative control microRNA inhibitor (anti miRs NC) or a pool of both miR-29a and miR-29b inhibitors (anti miRs 29ab) and silenced for both DNMT3A and B (siDNMT3s) or as control for GFP (siGFP). Protein amount was normalized by immunoblotting for CDK4 or tubulin, as indicated. Figures represent one indicative of three independent experiments. Statistically significant differences (*p < 0.05,**p < 0.01; n.s. no significance) for three independent experiments are reported.

strong *E-cadherin* repression nor *Mmp9* and *Vimentin* induction (Fig. 4B).

Finally, we aimed to clarify whether ectopic expression of mir-29 impacts EMT. Notably, as shown in Fig. 5A–B–C, the overexpression of a mir-29b precursor in hepatocytes undergoing tgfβ-induced EMT impeded the acquisition of the mesenchymal phenotype (i.e. induction of Snail and MMP9 and downregulation/delocalization of E-cadherin) and this was paralleled by the interference with DNMT3s and Snail up regulation.

Moreover, we analyzed the effects of endogenous mir-29a and mir-29b knock down. In cells treated with a pool of specific mir-29a and mir-29b inhibitors (antimirs 29ab), DNMT3s proteins were found positively modulated and this effect was counteracted by DNMT3A and B silencing (Fig. 5D). It's worth noting that, since the DNMT3A simultaneous interference induces, *per se*, higher DNMT3B levels (Fig. 5D and data not shown), the DNMT3B silencing in the presence of control anti-mir is not detectable.

With respect to the transition, mir-29 a and mir-29b inhibitors treatment induced the expression of the EMT master regulator Snail; notably, this effect was opposed by DNMT3s silencing (Fig. 5D); transcript levels of others EMT markers (e.g. MMP9, Vimentin and E-Cadherin) were found not significantly affected (data not shown).

Overall these results suggest a functional role for DNMT3s in the upregulation of EMT master factor Snail thus suggesting the need for DNMT3s repression in differentiated cells; presented data also indicate HNF4α as a conceivable executor of this repressive role through the regulation of miRNAs-29 targeting DNMT3s.

4. Discussion

In the current study, we provide evidence for a molecular mechanism functionally linking a master regulator of EMT/MET dynamic, namely HNF4α, to the epigenetic modifications featured by *de novo* DNA methylation.

Molecular mechanisms triggering and controlling EMT/MET dynamics have been so far only partially unveiled. In particular, the main effort has been dedicated to the identification of transcriptional regulators; the EMT main effectors have been indeed identified in transcriptional repressors (i.e. Snail, Slug, ZEB) targeting several epithelial genes [23]; conversely, a few master factors have been functionally linked to the MET acting by the down regulation of EMT-inducing repressors and restoring tissue-specific epithelial identities.

Although the EMT/MET profound gene reprogramming conceivably implies an equally deep remodeling of epigenetic setting, only recent reports inform on key roles for epigenetic code modifications also in these transitions [24–27]. Moreover, the possibility that master effectors of EMT and MET might directly impact the epigenetic modifications underlying these complex phenomena is still largely unexplored. Here, we extend the "to date" unveiled HNF4α activities to the capacity to influence epigenetic modifications performed by DNMT3s.

The liver-enriched transcriptional factor HNF4α is a well-known master factor of MET [13,28–31] initially characterized as a positive regulator of transcription of epithelial genes and recently reported to act also as a direct repressor of mesenchymal genes and master EMT-regulators [16]. Herein, using both cell culture and liver-specific *Hnf4α* knockout mouse models, we demonstrated a direct correlation between loss of HNF4α and up-regulation of DNMT3B, which supports a functional role during *Hnf4a*-mediated epigenetic remodeling. With respect to DNMT3A, *in vivo* data indicated up regulation in only half of the animals analyzed and we consider the data to have a statistical value only for the cellular model.

Notably, HNF4α impairment causes the negative regulation of miR-29a and miR-29b, targeting DNA methyltransferase transcripts. Concerning mechanisms, we provided evidence for HNF4α binding to miR-29a and miR-29b common promoter thus suggesting as HNF4α could regulate DNMT3A and DNMT3B abundance in hepatocytes through miRs-29 regulation; further experiments are required to support the here suggested central and direct role of HNF4α. Our evidence for a miRNA-mediated control of EMT/MET dynamics are in line with previous evidence regarding miR-34/Snail/HNF4α and the miR-200/Snail/Zeb circuits [32,33], thus highlighting a key role for miRNAs in the fine tuning of gene expression that guarantees cellular plasticity. Further studies are required to clarify whether the here proposed post-transcriptional mechanism of miRs-29 regulation by HNF4α is paralleled by an HNF4α-mediated DNMT3s transcriptional control.

Finally, we have shown that the rearrangement of DNA methylation pattern is required to fulfill EMT: treatment with 5-Azacytidine inhibitor, indeed, impeded the acquisition of the mesenchymal phenotype by TGFβ-treated hepatocytes, consistent with the observation that Snail was not induced and, coherently, E-cadherin was still retained at the membrane. Notably, miR-29b precursor overexpression interfered with the TGFβ-induced Snail up regulation and with the loss of epithelial phenotype. Conversely, treatment with both miR-29a and -29b specific inhibitors caused Snail induction and, of note, this effect is impaired by DNMT3 silencing. This demonstrates the significance of the miRs-29-DNMT3 mechanism in controlling EMT. Interestingly, a recent report by Parpart and colleagues [34] correlated low levels of miR-29 and DNMT3A induction to aggressiveness of HCCs. This is in line with the observations by Kogure *et al* [20], showing the involvement of miR-29a in DNMT control in HCC cells. Further studies will be necessary to evaluate a possible direct role of miRs-29 in Snail regulation.

5. Conclusions

In conclusion, from our data it emerges the functional role for DNMTs in the execution of the EMT thus highlighting the need for their repression in differentiated cells.

Our results suggest also the HNF4α-miRNAs-29 axis as a possible mediator of this repression; thus the negative control of *de novo* DNA methylation activities could be included among the HNF4α-mediated effects conferring histo-specificity.

Further understanding of the mechanism by which HNF4α impairs epigenetic remodeling mediated by DNA methylation will hopefully be instrumental for further research on reprogramming and ultimately for cell therapies in late stages of hepatocyte tumorigenesis.

Transparency document

The Transparency document associated with this article can be found, in the online version.

Acknowledgments

We thank Franca Citarella for suggestions and editing of the manuscript and Federica Astorri for technical assistance.

Grant Support: Associazione Italiana per la Ricerca sul Cancro (*IG 14114*); Ministry for Health of Italy ("*Ricerca Corrente*"); Ministry of University and Scientific Research of Italy (*PRIN 2010LC747T_003*).

References

[1] H. Acloque, M.S. Adams, K. Fishwick, et al., Epithelial–mesenchymal transitions: the importance of changing cell state in development and disease, J. Clin. Invest. 119 (6) (2009 Jun) 1438–1449.
[2] A. Jeltsch, Beyond Watson and Crick: DNA methylation and molecular enzymology of DNA methyltransferases, Chembiochem 3 (4) (2002 Apr 2) 274–293.
[3] S. Pradhan, P.O. Esteve, Mammalian DNA (cytosine-5) methyltransferases and their expression, Clin. Immunol. 109 (1) (2003 Oct) 6–16.
[4] M. Okano, D.W. Bell, D.A. Haber, et al., DNA methyltransferases Dnmt3a and Dnmt3b are essential for de novo methylation and mammalian development, Cell 99 (3) (1999 Oct 29) 247–257.
[5] Y. Saito, S. Hibino, H. Saito, Alterations of epigenetics and microRNA in hepatocellular carcinoma, Hepatol. Res. 44 (1) (2014 Jan) 31–42.
[6] Y. Saito, Y. Kanai, M. Sakamoto, et al., Expression of mRNA for DNA methyltransferases and methyl-CpG-binding proteins and DNA methylation status on CpG islands

and pericentromeric satellite regions during human hepatocarcinogenesis, Hepatology 33 (3) (2001 Mar) 561–568.
[7] M.A. Song, M. Tiirikainen, S. Kwee, et al., Elucidating the landscape of aberrant DNA methylation in hepatocellular carcinoma, PloS one 8 (2) (2013) e55761, http://dx.doi.org/10.1371/journal.pone.0055761 (Epub 2013 Feb 20).
[8] W. Ding, H. Dang, H. You, et al., miR-200b restoration and DNA methyltransferase inhibitor block lung metastasis of mesenchymal-phenotype hepatocellular carcinoma, Oncogenesis 1 (2012) e15, http://dx.doi.org/10.1038/oncsis.2012.15.
[9] Y. Chen, K. Wang, R. Leach, 5-Aza-dC treatment induces mesenchymal-to-epithelial transition in 1st trimester trophoblast cell line HTR8/SVneo, Biochem. Biophys. Res. Commun. 432 (1) (2013 Mar 1) 116–122.
[10] M. Lombaerts, T. van Wezel, K. Philippo, et al., E-cadherin transcriptional downregulation by promoter methylation but not mutation is related to epithelial-to-mesenchymal transition in breast cancer cell lines, Br. J. Cancer 94 (5) (2006 Mar 13) 661–671.
[11] U. Bedi, V.K. Mishra, D. Wasilewski, et al., Epigenetic plasticity: a central regulator of epithelial-to-mesenchymal transition in cancer, Oncotarget 5 (8) (2014 Apr 30) 2016–2029.
[12] F.J. Carmona, V. Davalos, E. Vidal, et al., A comprehensive DNA methylation profile of epithelial-to-mesenchymal transition, Cancer Res. 74 (19) (2014 Oct 1) 5608–5619.
[13] F. Parviz, C. Matullo, W.D. Garrison, et al., Hepatocyte nuclear factor 4alpha controls the development of a hepatic epithelium and liver morphogenesis, Nat. Genet. 34 (3) (2003 Jul) 292–296.
[14] M.A. Battle, G. Konopka, F. Parviz, et al., Hepatocyte nuclear factor 4alpha orchestrates expression of cell adhesion proteins during the epithelial transformation of the developing liver, Proc. Natl. Acad. Sci. U. S. A. 103 (22) (2006 May 30) 8419–8424.
[15] C. Cicchini, L. Amicone, T. Alonzi, et al., Molecular Mechanisms Controlling the Phenotype and the EMT/MET Dynamics of Hepatocyte, 2014.http://dx.doi.org/10.1111/liv.12577 (Liver Int Online First: 25 April).
[16] L. Santangelo, A. Marchetti, C. Cicchini, et al., The stable repression of mesenchymal program is required for hepatocyte identity: a novel role for hepatocyte nuclear factor 4alpha, Hepatology 53 (6) (2011 Jun) 2063–2074.
[17] M. Fabbri, R. Garzon, A. Cimmino, et al., MicroRNA-29 family reverts aberrant methylation in lung cancer by targeting DNA methyltransferases 3A and 3B, Proc. Natl. Acad. Sci. U. S. A. 104 (40) (2007 Oct 2) 15805–15810.
[18] L. Amicone, F.M. Spagnoli, G. Spath, et al., Transgenic expression in the liver of truncated Met blocks apoptosis and permits immortalization of hepatocytes, EMBO J. 16 (3) (1997 Feb 3) 495–503.
[19] C. Cicchini, D. Filippini, S. Coen, et al., Snail controls differentiation of hepatocytes by repressing HNF4alpha expression, J. Cell. Physiol. 209 (1) (2006 Oct) 230–238.
[20] T. Kogure, Y. Kondo, E. Kazaku, et al., Involvement of miRNA-29a in epigenetic regulation of transforming growth factor-β-induced epithelial–mesenchymal transition in hepatocellular carcinoma, Hepatol. Res. 44 (2014) 907–919.
[21] A.M. Cozzolino, T. Alonzi, L. Santangelo, et al., TGFbeta overrides HNF4alpha tumor suppressing activity through GSK3beta inactivation: implication for hepatocellular carcinoma gene therapy, J. Hepatol. 58 (1) (2013 Jan) 65–72.
[22] J.K. Christman, 5-Azacytidine and 5-aza-2′-deoxycytidine as inhibitors of DNA methylation: mechanistic studies and their implications for cancer therapy, Oncogene 21 (35) (2002 Aug 12) 5483–5495.
[23] A. Cano, M.A. Perez-Moreno, I. Rodrigo, et al., The transcription factor snail controls epithelial–mesenchymal transitions by repressing E-cadherin expression, Nat. Cell Biol. 2 (2) (2000 Feb) 76–83.
[24] S. Javaid, J. Zhang, E. Anderssen, et al., Dynamic chromatin modification sustains epithelial–mesenchymal transition following inducible expression of Snail-1, Cell Rep. 5 (6) (2013 Dec 26) 1679–1689.
[25] O.G. McDonald, H. Wu, W. Timp, et al., Genome-scale epigenetic reprogramming during epithelial-to-mesenchymal transition, Nat. Struct. Mol. Biol. 18 (8) (2011 Aug) 867–874.
[26] K.J. Wu, M.H. Yang, Epithelial–mesenchymal transition and cancer stemness: the Twist1-Bmi1 connection, Biosci. Rep. 31 (6) (2011 Dec) 449–455.
[27] R. Li, J. Liang, S. Ni, et al., A mesenchymal-to-epithelial transition initiates and is required for the nuclear reprogramming of mouse fibroblasts, Cell Stem Cell 7 (1) (2010 Jul 2) 51–63.
[28] H. Chiba, T. Gotoh, T. Kojima, et al., Hepatocyte nuclear factor (HNF)-4alpha triggers formation of functional tight junctions and establishment of polarized epithelial morphology in F9 embryonal carcinoma cells, Exp. Cell Res. 286 (2) (2003 Jun 10) 288–297.
[29] N.L. Lazarevich, O.A. Cheremnova, E.V. Varga, et al., Progression of HCC in mice is associated with a downregulation in the expression of hepatocyte nuclear factors, Hepatology 39 (4) (2004 Apr) 1038–1047.
[30] G.F. Spath, M.C. Weiss, Hepatocyte nuclear factor 4 provokes expression of epithelial marker genes, acting as a morphogen in dedifferentiated hepatoma cells, J. Cell Biol. 140 (4) (1998 Feb 23) 935–946.
[31] S. Sekiya, A. Suzuki, Direct conversion of mouse fibroblasts to hepatocyte-like cells by defined factors, Nature 475 (7356) (2011 Jul 21) 390–393.
[32] M. Lu, M.K. Jolly, H. Levine, et al., MicroRNA-based regulation of epithelial-hybrid-mesenchymal fate determination, Proc. Natl. Acad. Sci. U. S. A. 110 (45) (2013 Nov 5) 18144–18149.
[33] F. Garibaldi, C. Cicchini, A. Conigliaro, et al., An epistatic mini-circuitry between the transcription factors Snail and HNF4alpha controls liver stem cell and hepatocyte features exhorting opposite regulation on stemness-inhibiting microRNAs, Cell Death Differ. 19 (6) (2012 Jun) 937–946.
[34] S. Parpart, S. Roessler, F. Dong, et al., Modulation of miR-29 expression by alpha-fetoprotein is linked to the hepatocellular carcinoma epigenome, Hepatology 60 (3) (2014 Sep) 872–883.